Journal of Astronomy and Space Sciences, Vol.1, 1984.

Aerodynamic Problems of Launch Vehicles

Kyong Chol Chou

Department of Space Science, Kyung Hee University
(Received July 10, 1984)

Abstract

The airflow along the surface of a launch vehicle together with base flow of clustered nozzles cause problems which may affect the stability or efficiency of the entire vehicle.

The problem may occur when the vehicle is on the launching pad or even during flight.

As for such problems, local steady-state loads, overall steady–state loads, buffet, ground wind loads, base heating and rocket–nozzle hinge moments are examined here specifically.

I. INTRODUCTION

Figure 1 indicates the subject under discussion–the aerodynamic problems of launch vehicles–and provides an orientation for the subject. Aerodynamics is shown as the hub of a wheel which has three spokes. The spokes are attached to the rim at points labeled inertia, elasticity, and heat.

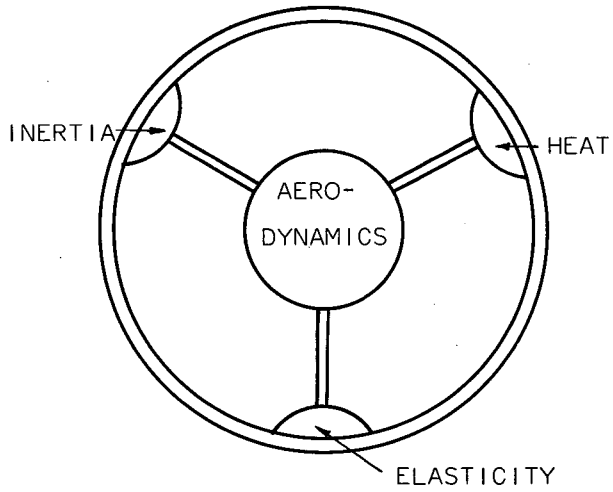

Fig. 1. Aerodynamic problems of launch vehicles

Aerodynamics alone and in combination with one or more of the items shown on the rim represents separate areas of investigation wherein the airflow about a launch vehicle may be an important factor. For example, the different spokes represent the areas of dynamics, aeroelasticity, and aerothermodynamics. The whole wheel represents the broad area of aerothermolasticity.

A very large number of specific problems are represented by this diagram. Only a few of the problems, as shown figure 2, have been chosen for discussion herein. A typical large launch vehicle is shown at the right of the figure. The treatment is directed more toward the problems of large launch vehicles than toward small ones; however, much of the discussion also applies to small launch vehicles.

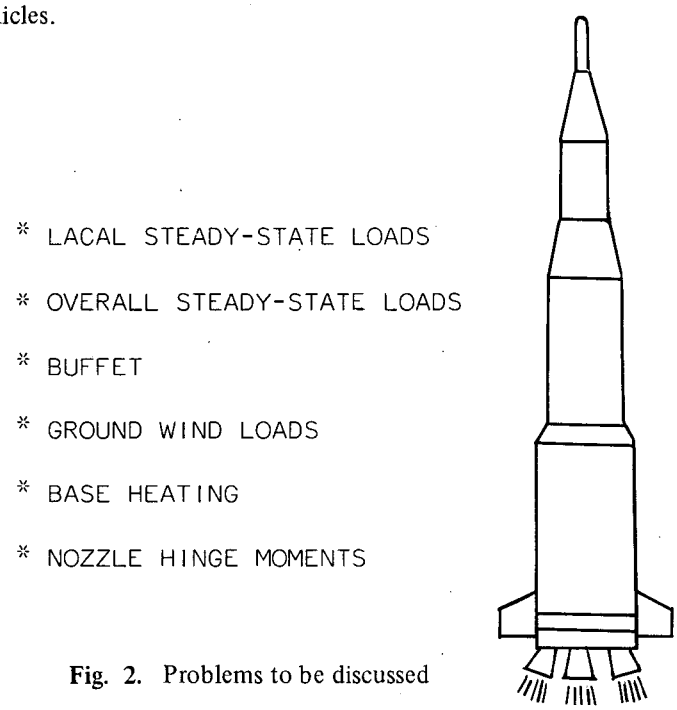

Fig. 2. Problems to be discussed

SYMBOLS

C_p	pressure coefficient, $\frac{p-p_\infty}{q}$
$C_{p,\text{peak}}$	peak negative pressure coefficient
f	frequency
M	Mach number local static pressure
p	local static pressure
p_∞	free–stream static pressure
q	free–stream dynamic pressure
$\bar{V}(x)$	steady wind velocity
$V(x.t)$	unsteady wind velocity
V_{WIND}	horizontal wind velocity

α angle of attach

σ_M root–mean–square bending moment

ϕ power=speetral density

II. LOCAL STEADY-STATE LOADS

The first subject to be discussed is local steady-state aerodynamic loads. Figure 3 shows the distribution of pressure coefficients over a typical vehicle. The Mach number is 1.3 and the angle of attack is zero. Negative pressure coefficients, which indicate pressures below ambient, are shown above the horizontal axis.

Note that large changes in pressure occur in the regions of the flares. Both negative and positive pressure-coefficient peaks are obtained, and these peaks represent concentrated local loads. The negative pressure-coefficient peaks occur at each corner where the flow is required to expand.

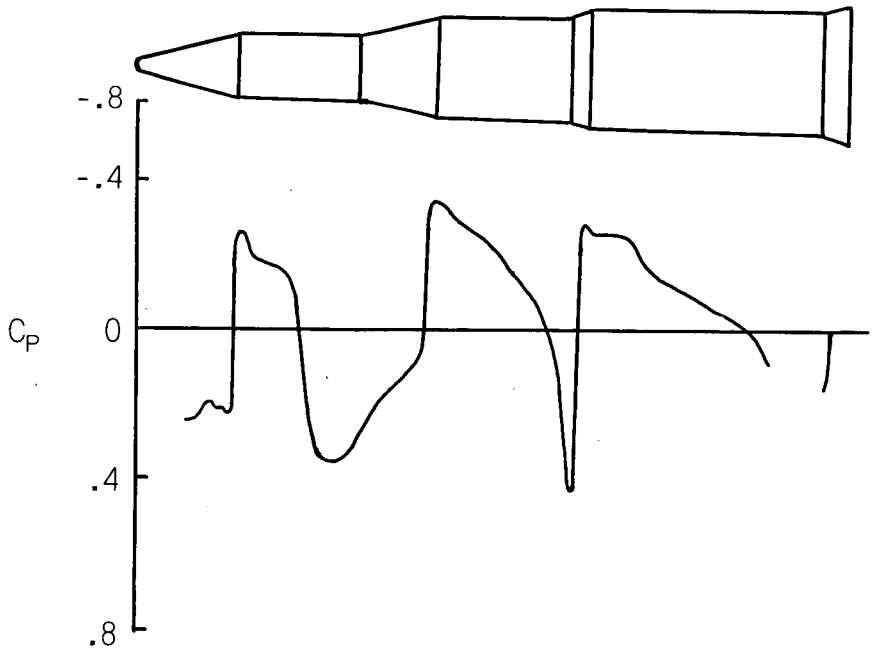

Fig. 3. Pressure distribution M=1.3; $\alpha = o^\circ$

The peak negative pressure coefficient near the first corner of a different nose cone is shown as a function of Mach number in figure 4. The dynamic pressure is also shown as a function of Mach number for a typical trajectory. The local load is proportional to the product of C_p and q as shown by the solid curve. It may be seen that the local load at a Mach number of 0.8 is about four times higher than the load at maximum dynamic pressure.

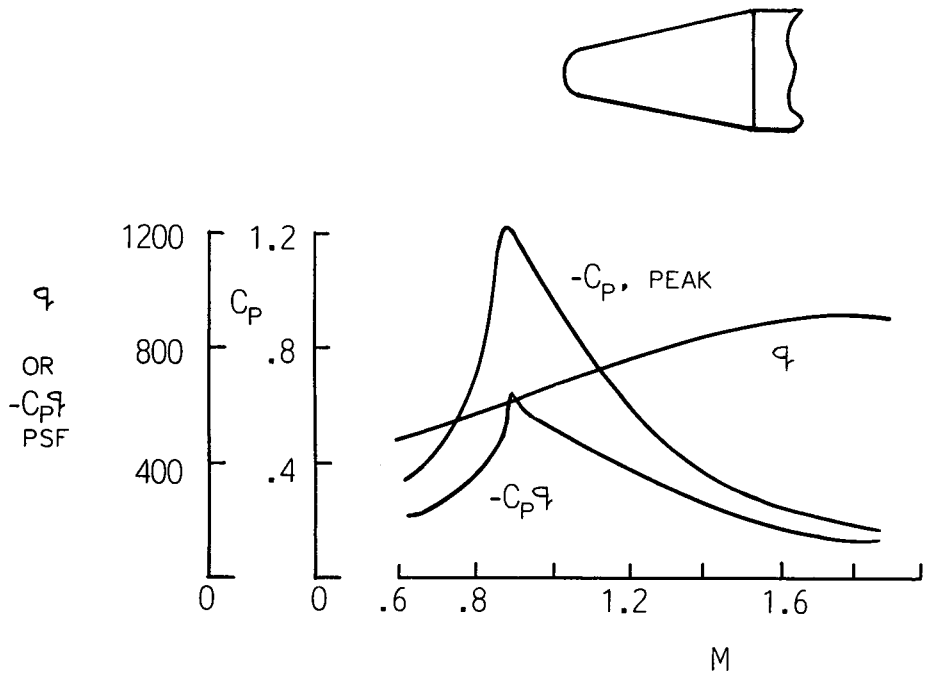

Fig. 4. Maximum local load for typical conecylinder

The local load is a particularly important factor in the design of secondary structures. Such as insulation panels or fairings. Several vehicle failures have occurred because local loads near a corner were underestimated. The assumption has been made in several instances that all aerodynamic loads are a maximum at the maximum dynamic-pressure condition. These data indicate the error of such an assumption.

Figure 5 again shows the variation of pressure coefficient with Mach number. The configuration is a cone-cylinder. During launch the March number continually increases and the Mach number scale may be thought of as a time scale. Maximum negative pressure coefficients at transonic speeds occur near the corner as indicated by the solid curve. In interstage sections of launch vehicles and also in adapter sections behind payloads, of which this configuration might be an example, the volume enclosed is often vented to the external flow. A vent located at the corner, at point A, might reduce the local load across the skin at point A to very low values. However, it may be seen that if the internal pressure is maintained at the value plotted here for point A, the net pressure difference across the skin at point B would be the difference between the two curves, and the local loads might become large at point B. Thus in the very important problem of locating vents, a detailed knowledge of the variation of the pressure with Mach number is required.

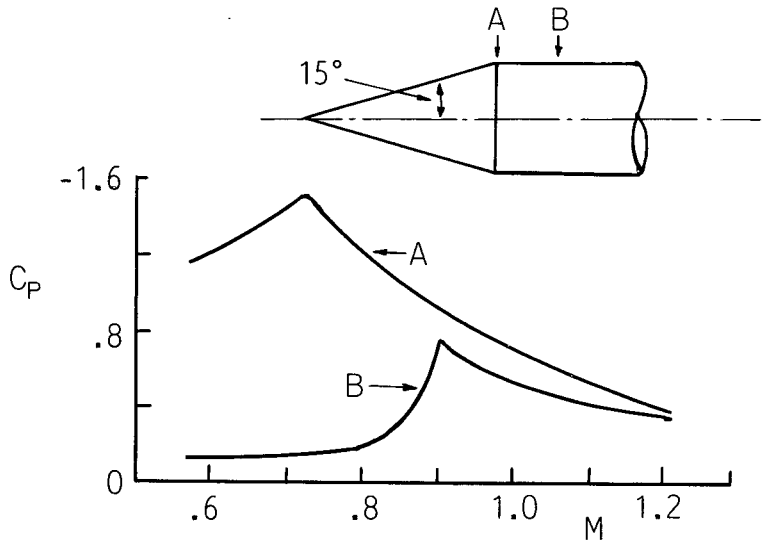

Fig. 5. Local load for cone-cylinder

III. OVERALL STEADY-STATE LOADS

Figure 6 introduces the subject of overall steady-state loads. The Mach number and dynamic pressure are plotted as functions of altitude for an example trajectory. The velocity of horizontal winds which the vehicle might encounter is shown also as a function of altitude. This variation of wind velocity with altitude is about an average of the different profiles used for design purposes (Runyan *et al*, 1962). The response of an elastic vehicle to varying horizontal winds is discussed briefly in reference 1; in the present paper, only the steady-state aspects of the problem are considered.

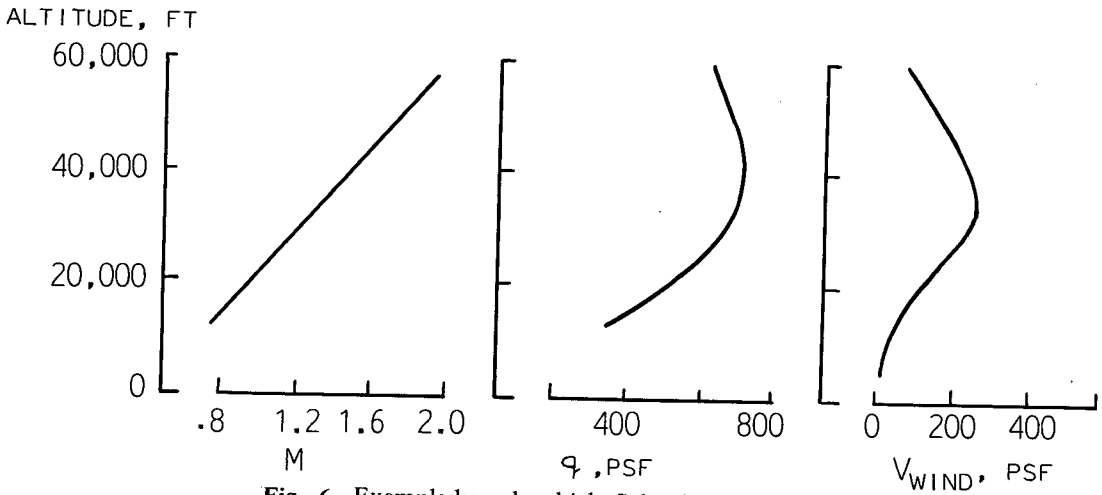

Fig. 6. Example launch-vehicle fight characteristics

The horizontal winds cause the vehicle to fly at an angle of attack. Note that the maximum dynamic pressure occurs at about the same altitude as the maximum horizontal winds so that the maximum dynamic pressure and maximum angle of attack occur at about the same time. As will be shown subsequently, the effect of angle of attack is to produce a bending moment along the vehicle lenght. The bending moment is nearly proportional to the product of dynamic pressure and angle of attack so that the maximum bending moments will be obtained in this region. The Mach number for large launch vehicles is usually between 1.5 and 2.0. The is a very important load condition for the design of the vehicle structure. Thus, maximum bending moments generally occur at supersonic Mach numbers, and maximum local loads (discussed previously) usually occur at high suhsonic Mach numbers.

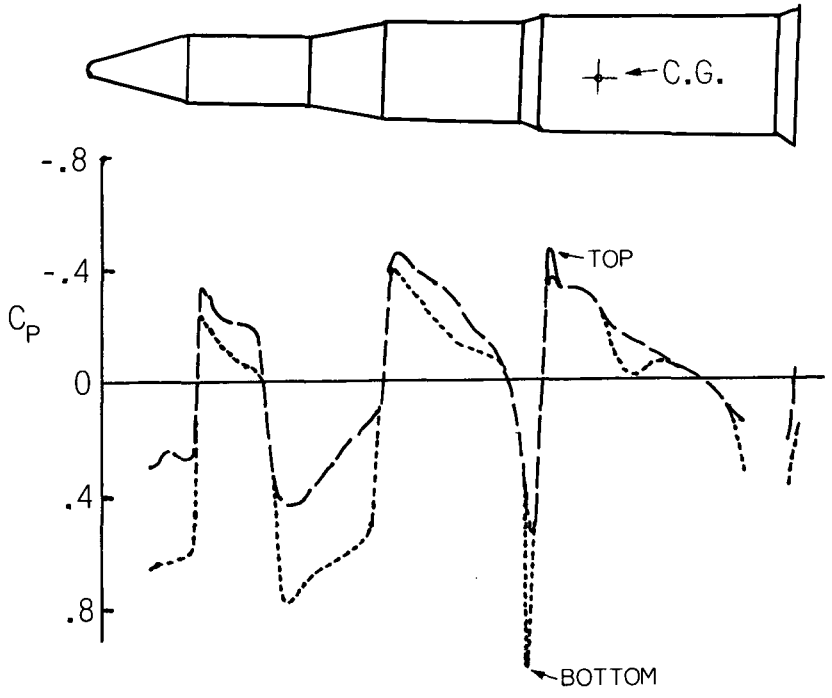

Fig. 7. Pressure distribution M=1.3; $\alpha = 8^\circ$

Figure 7 shows the pressure distribution obtained on a vehicle at an angle of attack of 8° for the top and bottom surfaces. As just discussed, the angle of attack might be caused by horizontal winds. The vehicle shown in figure 7 is the same as that shown in figure 3 and the Mach number again is 1.3. These data indicate that at each point along the vehicle length there is an upward force on the vehicle. To calculate the pitching-moment distributions along the vehicle length, the vertical component of the pressure force is integrated circumferentially and logitudinally. Typically, for a vehicle without fins at the base, a nose-up pitching moment is obtained

about the vehicle center of gravity for positive angles of attack. The pitching moment is counteracted by the stabilization system, which for example, might be swiveling rocket nozzles. The two opposing moments produced the bending moment in the vehicle.

Thus, accurate determination of the bending-moment distribution, as well as local loads discussed previously, requires an accurate determination of the pressure distribution. No completely satisfactory theoretical method exists for computing the pressure distributions throughout the required Mach number and angle-of-attack ranges. Slender-body, shock–expansion, and piston theories give trends for some conditions, but the theoretical treatment is grossly inadequate. In practice, most designers have a collection of load distributions obtained experimentally for various shapes, and these data are used in preliminary design. For final verification, wind-tunnel studies of the configuration are often made and add more data to the collection. A much more satisfactory situation would be to have a reliable theoretical method of predicting pressure, particularly at transonic speeds.

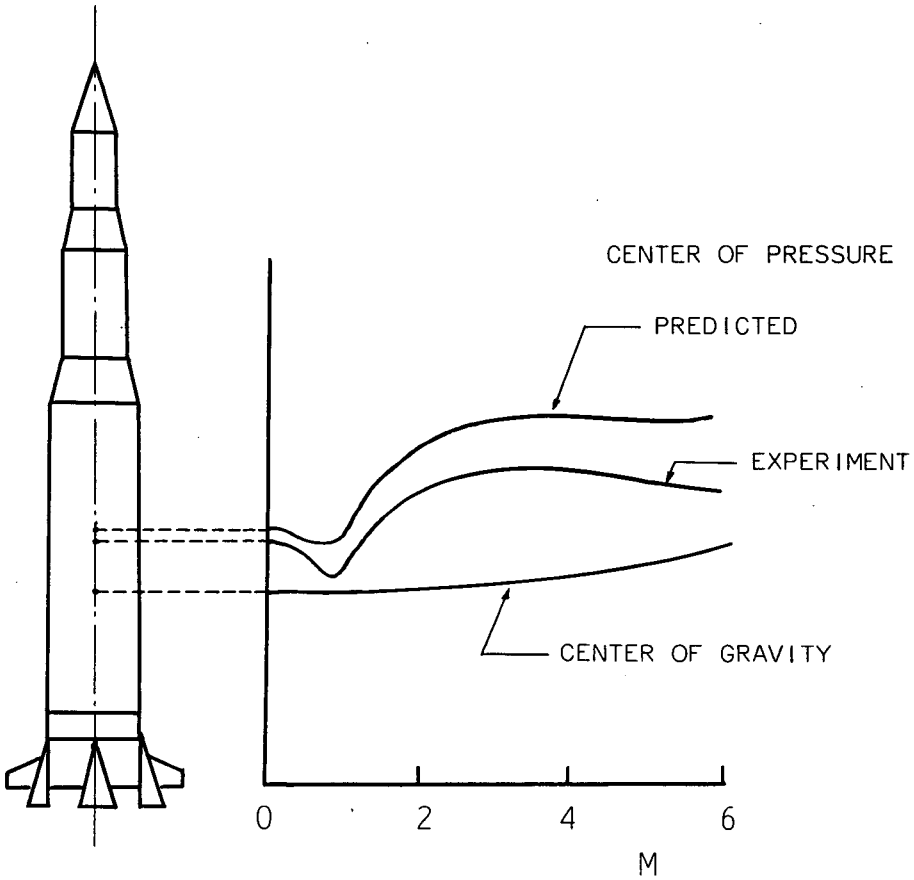

Fig. 8. Static stability

Figure 8 illustrates another aspect of the need for accurate prediction of the pressure distributions. A typical vehicle is shown at the left of the figure. The upper curve is the predicted center-of- pressure location on the vehicle obtained by use of theory and the generalized experimental data available. The middle curve is the center-of-pressure location as measured in wind-tunnel studies. The center of gravity of the vehicle, shown by the bottom curve, varies with burning time.

With center of pressure ahead of the center of gravity, the vehicle is aerodynamically unstable. It may be seen that somewhat greater instability was predicted than was measured. An engine–swiveling requirement for automatic stabilization, based on the analytical prediction, would yield a considerably conservative design. The problem of attitude stabilication for large guided vehicles is discussed in Geissler (1960).

IV. BUFFET

Buffet is simply pressure oscillations caused by separated flow. The greatest buffet problems occur at transonic speeds where shock interactions with the seperated flow augment the pressure fluctuations. Often buffet produces the greatest loads at the same loads at the same locations and conditions where the local steady-state loads are a maximum. Three types of buffet which have been observed are shown in figure 9.

Shock-boundary-layer interaction buffet is often obtained on hamerhead configurations of the type shown. The flow resembles that over thick airfoils at transonic speeds.

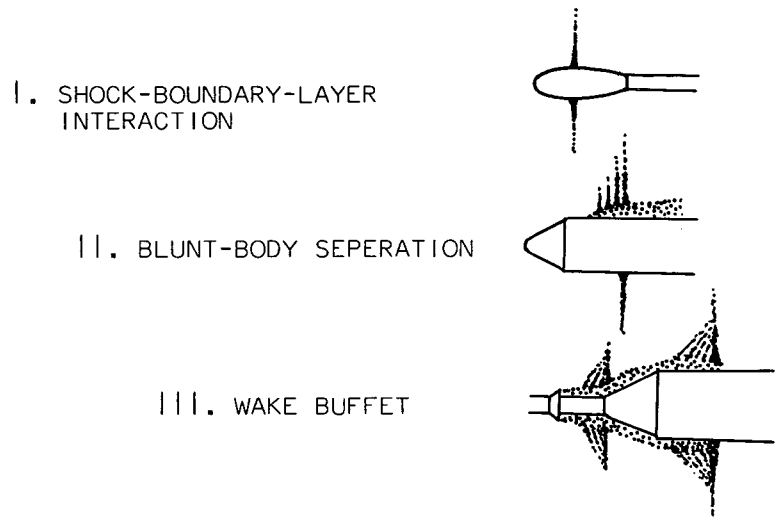

Fig. 9. Types of buffet flow on launch vehicles

Blunt-body separation buffet is characterized by unstable flow at the shoulder of a blunt conecylinder. At subsonic Mach numbers the flow is separated at the corner and at supersonic speeds it is attached. At Mach numbers just below one, the flow is alternately separated and attached.

Abrupt protuberances cause an unsteady wake which impinges on down-stream parts of the vehicle and causes wake buffet. It is this type of buffet which appears to have caused the failure of the first Mercury–Atlas vehicle. Subsequent vehicles were strengthened and no further structural problems have been encountered.

As shown in figure 10, different types of buffet may have considerably different characteristics. These power spectra of the pressures show that the energy of the wake buffet is distributed over the frequency range, while most of the shock-boundary-layer interaction buffet is concentrated at low frequencies. These two types of buffet would be expected to cause considerably different elastic responses of the structure. With the buffet energy concentrated at low frequencies, overall bending modes might be excited. With distributed buffet energy, local response of the structure might be excited. Before model buffet data such as these can be applied with confidence to full-size vehicles, the scaling relationships must be derived and verified experimentally. Simple dimentional considerations would indicate, for example, that the buffet frequency spectrum would be shifted to higher frequencies as the model scale is reduced. Buffet-pressure studies have been conducted with models which differed only in size, and the scaling laws based on the simple dimensional considerations appear to have been verified.

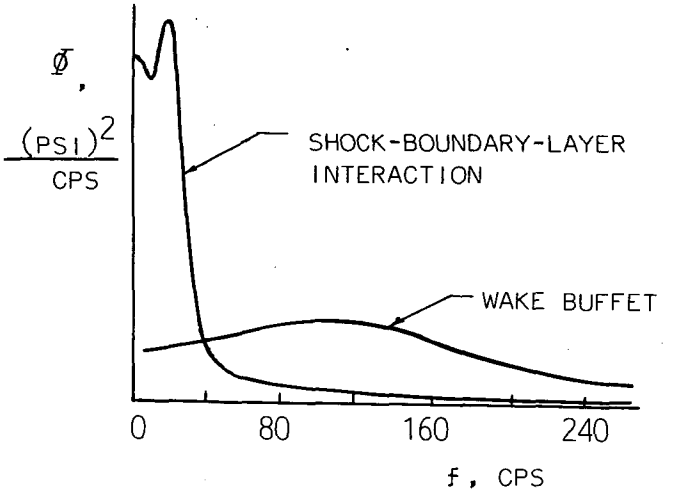

Fig. 10. Pressure power speetra; transonic wind-tunnel results

Since buffet is suspected to be the cause of several vehicle failures, a wind-tunnel study program on buffet pressures have been undertaken by several workers. coe (1981, 1962) present results obtained to date.) The value of this buffet-pressure program is well recognized; how-

ever, considerable difficulty exists in applying the buffet-pressure data to the structural design. The obvious approach is to use experimental buffet pressures as force inputs in a dynamic analysis of the structure; however, the task of obtaining sufficiently detailed experimental data and of making the calculations appears to be over whelming.

Figure 11 illustrates an alternate to such a response analysis. The two models Hanson *et al.* (1982.) are a hammerhead configuration and blunted conecylinder. The models had the same dynamic and elastic properties and were supported in a wind tunnel in such a way that they were free to in their elastic free-free bending modes. The response of the models was measured in terms of the root-mean-square bending moment as a function of Mach number. Thus, the aero-elastic models were used as windtunnel analogues to measure the response directly. The low-level response for the conecylinder model is believed to be caused primarily by winde-tunnel turbulence. The much higher level response of the hammerhead configuration is due to buffeting produced by the reflex frustum.

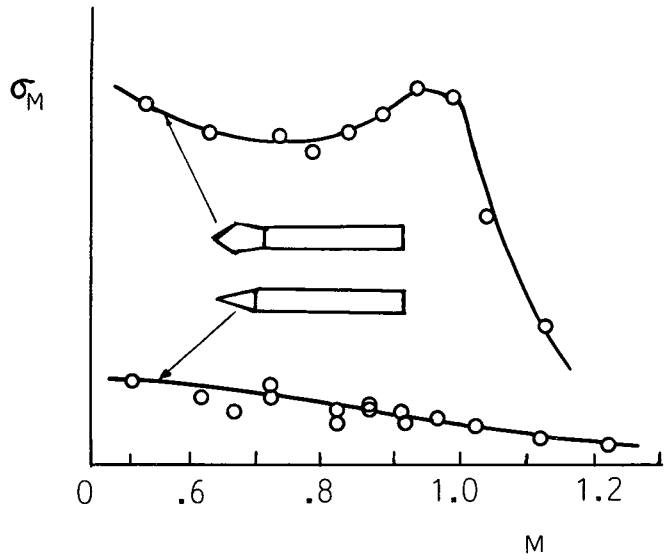

Fig. 11. Effect of nose shape on buffet response

Figure 12 shows the power spectra of the bending moment for the same two models at a Mach number of 0.90. Naturally, the data for the cone-cylinder model are at a very low level. Of considerable interest is that the response for the hammerhead configuration was primarily in the first two bending modes, and each mode contributed about equally to the total response. The technique of using aeroelastic models for buffet-response studies such as these has been used previously for aireaft wings Huston *et al* (1975). In aircraft wing models the simulation of only the first elastic wing mode usually sufficed. However, it appears from this result that at least two elastic modes must be simulated for launch-vehicle models.

To date no flight data have been available for correlation with the wind-tunnel response measurements. Correlation will have to be shown, of course, before the technique can be considered reliable for prediction on buffet response. It is anticipated that models might be satisfactory for predicting overall bending response; however, the prediction of localized response of panels might require structural replica models at small scale and might therefore be infeasible. Meanwhile, additional emphasis is needed on analytical solution of the buffet loads, using power-spectral approaches for very simple shapes.

Figure 12 may also be referred to in connection with another aspect of vehicle response. The sharpness of the peack indicates that the total of the structural and aerodynamic damping was low for both modes. In fact, negative aerodynamic damping was measured in the first mode at slightly greater Mach numbers, and this situation is of concern because of the possibility that sustained or divergent oscillations of the vehicle may be produced. However, in most applications, the magnitude of any negative aerodynamic damping is very small compared with the positive damping usually provided by the structure, the thrust-vector control system, and the liquid fuel so that sustained or divergent oscillations of the vehicle have not yet materialized as a major problem.

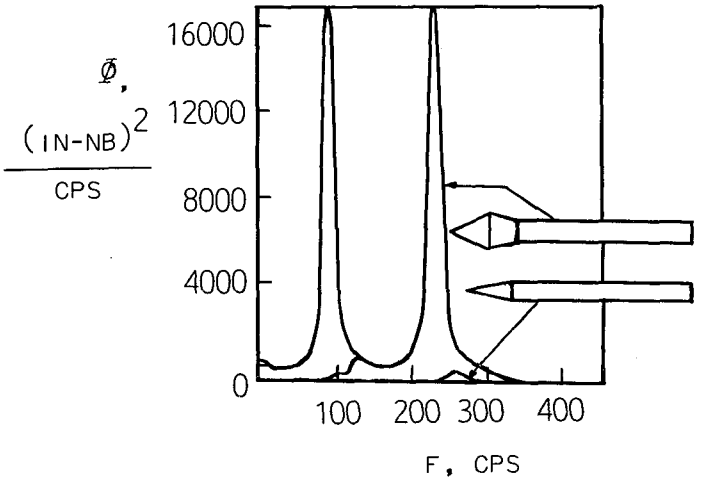

Fig. 12. Bending-moment power spectra M=0.90; $\alpha = 0°$

V. GROUND WIND LOADS

The ground wind-loads problem is introduced in figure 13. The launch vehicle is shown on the launch pad during prelaunch operations. The horizontal wind is considered to consist of a steady wind vector which varies both with time and with height above the ground. The unsteady part is due to gusts and trubulence. The winds produce a steady drag deflection and oscillatory

deflections in both the lateral and drag directions. The deflections cause problems in strural strength, guidance alinement, and flight-instrumentation checkouts. The problem is of sufficient importance that design or operations changes have been required for several vehicles.

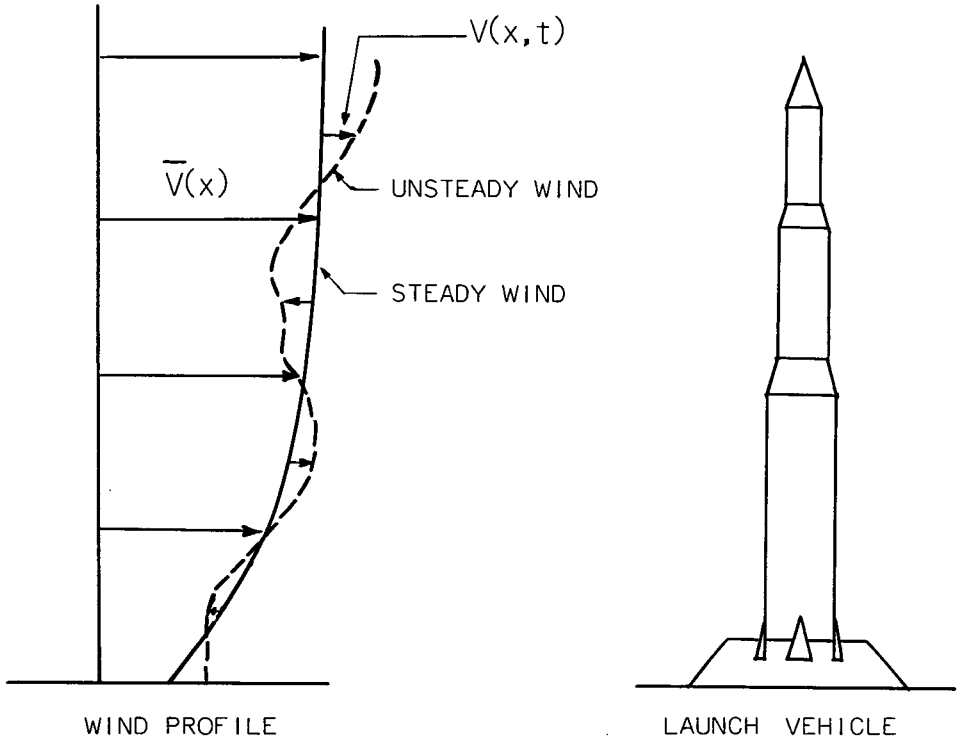

Fig. 13. Launch vehicle exposed to ground winds

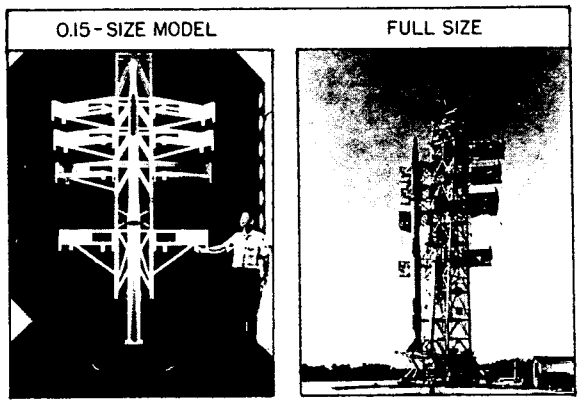

Fig. 14. Scout vehicles

The oscillatory lateral deflections are caused primarily by the steady wind vector and no satisfactory analytical technique exists for predicting the input aerodynamics, even for twodimensional cyliders. Wind-tunnel studies of models Buell and Kenyon (1959) and Ezra and Birnbaum (1980) are therefore required for lateral load predictions. Figure 14 shows such a model used in Jones and Gilman (1961). On the right is shown the Scout vehicle and on the left, the dynamically and elastically scaled 15-percent wind-tunnel model. The model, complete with simulated launch tower, is shown mounted in the wind tunnel. The accurary with which ground wind response to steady winds can be simulated in wind tunnels is a moot question because of a lack of response data on full-scale vehicles which could be used for comparison with wind-tunnel data. Thus, a need exists for improving the analytical prediction methods for steady winds and for obtaining response data for full-scale vehicles.

The oscillatory drag deflections, caused primarily by the unsteady wind vector, can probably be handled analytically by using power-spectral density techniques Bohne (1982). The handicap has been the lack of power spectra information on winds near the ground. The small amount of data available have been obtained, for the most part, with conventional wind-measuring devices which are not responsive to the higher wind frequencies that can represent important dynamic load inputs to the vehicle. Thus, a need exists to determine the ground-wind properties in greater detail. A fast response anemomenter under development for this purpose is described in Reed and Lynch (1972).

VI. BASE HEATING

Figure 15 illustrates the base-heating problem Schueller (1979) Goethert (1981, 1961), and Beheim (1982). The base of a launch vehicle which has a cluster of four rocket nozzles is shown. At high altitudes the rocket exhausts plume and intersect. Trailing shock waves are

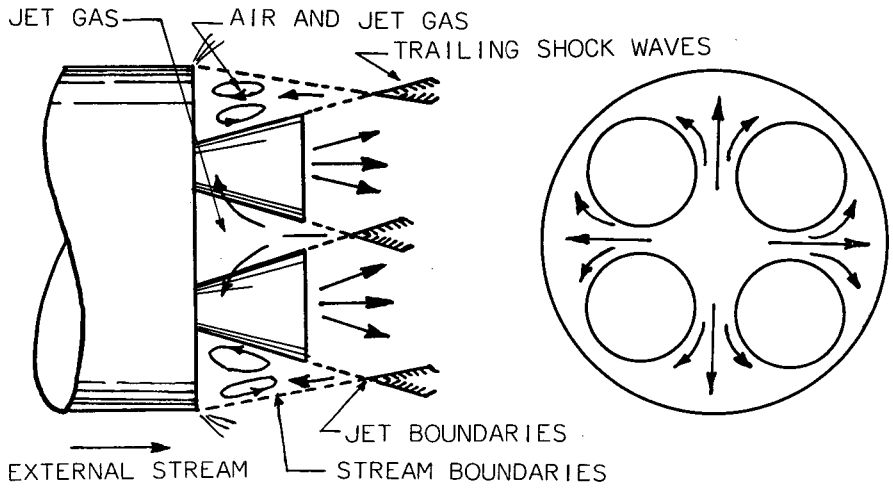

Fig. 15. Base flow for clustered nozzies

formed at the intersection of the jets. The energy of the air near the jet boundaries is too low to allow the flow to move back through the shock waves, so the flow reverses and flows toward the base of the vehicle. It escapes by flowing laterally across the base. At high altitudes, this recirculated flow of hot exhaust gases reaches supersonic velocities and can cause severe damage to surfaces which are not heat protected.

The intersection of the jet exhaust with the external stream also produces trailing shock waves and a reversed flow. In this case, oxygen from the external stream combined with the fuel-rich exhaust produces a combustible mixture which could lead to burning in the base region. A much more likely source of base burning, however, is from the exhaust of the turbines which pump the propellants, since the turbine exhaust is even more fuel-rich than the rocket jets.

The significance of the sources of base beating as a function of altitude in miles is shown qualitatively in figure 16. This figure is based on information from Goethert (1961). Recirculation of the hot exhaust gases is indicated to be a major problem into space. At lower altitudes the jets plume less, the trailing shock strength decreases, and less of the hot gases is recirculated. At still lower altitudes, the jets do not instead as ejectors in pulling the external stream over the base to produce base cooling rater than heating. Base burning is indicated to be a major problem at altitudes from 3 to 10 miles. At higher altitudes, the lack of oxygen precludes combustion. Radiation is shown as the third source of base heating. Much of the radiation comes from afterburning of the rocket jet downstream of the nazzle.

Base-heating problems are generally studied by use of scaled models in wind tunnels and altitude chambers. Considerable work remains tobe done in improving model-testing techniques.

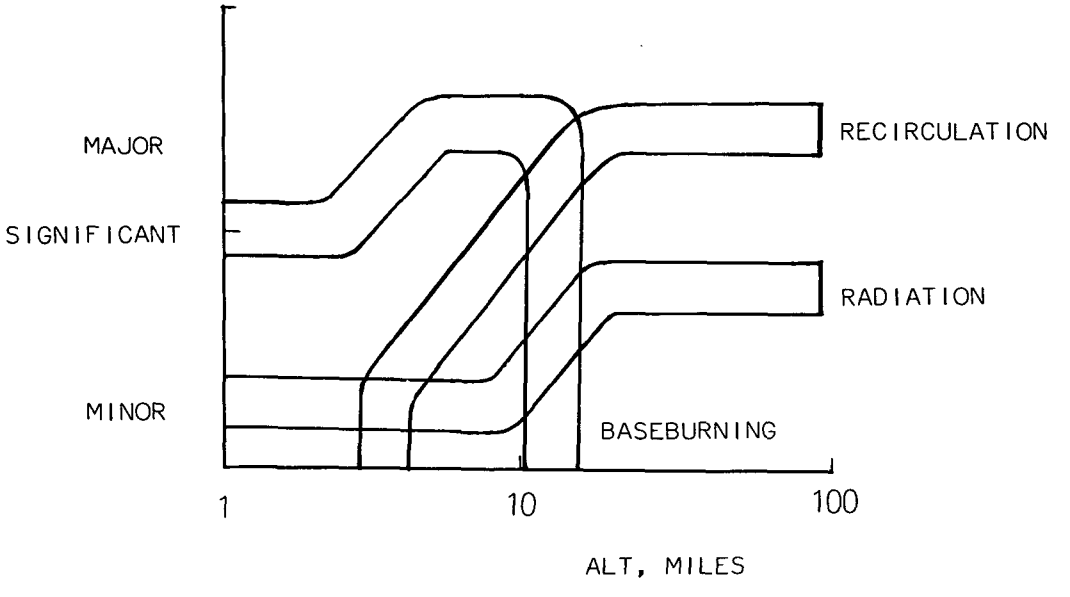

Fig. 16. Source of base heating for clustered nozzles

VII. NOZZLE HING MOMENTS

Figure 17 introduces the subject of the aerodynamic hinge moments on swiveling rocket nozzles. The bases of two Saturn vehicles are shown; both vehicles utilize swiveling nozzles to produce thrust-vector control.

For the C-1 Block 1 vehicle shown at the left, the H-1 engines are contained within the periphery of booster and relatively large shrouds extend over the nozzles. Consequently there is very little impingement of the external flow on the nozzles.

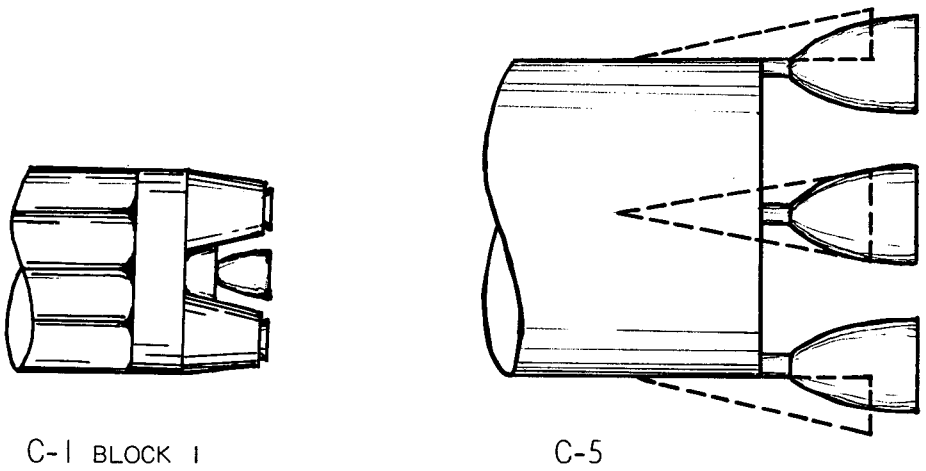

Fig. 17. Base regions of Saturn vehicles

However, with the C-5 vehicle, the center lines of the outer F-1 engine nozzles lie nearly on the booster periphery. If not shrouds are used, the external stream impinges on a large area of the nozzles. This impingement produces very large moments which lead to impractically large actuators in order to overcome the hinge moments. Elaborate backup structure would also be required for the actuator. Large shrouds may be used to shield the nozzles from the external flow, but the shroud loads then become large, and excessive backup structure is required for the shrouds. In addition, the base drag of the vehicle becomes large and the recirculation of exhaust gases at the base can become a serious problem. A probable solution is to use a shroud of moderate length, perhaps about as shown by the dashed lines, and to use scoops to guide airflow into the base area. A proper arrangement can reduce hinge moments as well as recirculation and base drag.

Wind-tunnel studies are used for predicting the nozzle hinge moments since present theories are inadequate for prediction of the complicated flow field behind the base of a launch vehicle. It would probably not be profitable to expend a great deal of effort in developing a theoretical method because the problem is so dependent on the details of the configuration and the operating

conditions. However, the problem is an interesting example of the many different kinds of aerodynamic problems encounted in the design of launch vehicles.

VIII. CONCLUSION

In conclusion, some of the aerodynamic problems of launch vehicles have been discussed. The importance of the problems has been sited and areas where additional work is required have been indicated.

The airflow about a launch vehicle causes problems which may affect the entire vehicle or may effect only localized areas; the problems can occur when the vehicle or may effect only localized areas; the problems can occur when the vehicle is on the launcher as well as during flight, Specific overall steady-state loads, buffet, ground wind loads, base heating, and rocket-nozzle hinge moments.

REFERENCES

Beheim, Milton A., and Obery, Leonard J.: Wind Tunnel Studies of Booster Base Heating. Paper no. 62-166, Inst. Aerospace Sci., June 1982.

Bohne, Quintin R. : Power Spectral Considerations on the Launch Pad. Proc. Nat. Symposium on Winds for Aerospace Vehicle Design. Vol. I. Air Force Surveys in Geophysics, No. 140 [AFCRL-62-273(I)], Mar. 1982.

Buell, Donald A., and Kenyon, George G.: The Wind-Induced Loads on a Dynamically Scaled Model of a Large Missile in Launching Position. NASA TM X-109, 1959.

Coe, Chables F.: Steady and Fluctuating Pressures at Transonic Speeds on Two Space-Vehicle Payload Shapes. NASA TM X-503, 1961.

Coe, Charles F.: The Effects of Some Variations in Launch-Vehicle Nose Shape on Steady and Fluctuating Pressures at Transonic Speeds. NASA TM X-646, 1962.

Ezra, A.A., and Birnbaum, S.,: Design Criteria for Space Vehicles To Resist Wind Induced Osciliations. (Preprint) 1071-80, American Rocket Soc., APR. 1980.

Geissler, Ernst D.: Problems in Attitude Stabilization of Large Guided Missiles. Aerospace Eng., vol. 19, no. 10, Oct. 1960, pp. 24-29. 68-71.

Goethert, B.H.: Base Flow Characteristics of Missiles With Cluster-Rocket Exhausts. Aero/Space Eng., vol. 20, no.3, Mar. 1981, pp. 28-29, 108-117.

Goethert, B.H.: Base Heating Problems of Missiles and Space Vehicles. (Preprint) 1666-61, American Rocket Soc., Mar. 1961.

Hanson, Perry W., and, Doggett, Roeert V., Jr.: Wind-Tunnel Measurements, of Aerodynamic Damping Derivatives of a Launch Vehicle Vibrating in Free-Free Bending Modes at Mach Numbers From 0.70 to 2.87 and Comparisons With Theory. NASA TN D-1391, 1982.

Huston, Wilber B., Rainey, A. Gerald, A. Gerald, and Baker, Thomas F.: A Study of the Correlation Between Flight and Wind-Tunnel Buffeting Loads. NACA RM L55E16b

1975.

Jones, George W., Jr. and Gilman, Jean, Jr.: Mrasured Response to Wind-Induced Dynamic Loads of a Full-Scale Scout Vehicle Mounted Vehicle Mounted Vertically on a Launching Tower. NASA TN D-757, 1961.

Reed, Wilmer H., III, and Lynch, James W.: A Simple Fast Response Anemomenter, Presented at Conference on Low Level Winds (El Paso-Dallas, Texas), Aug. 7-9, 1972. (Sponsored by the U.S. Army Missile Support Agency and the American Meteorological Soc.)

Runyan, Harry L., and Leonard, Robery W.: Research, Design Considerations, and Technological Problems of Structures for Launch Vehicles. NASA University Conference, 1962 (paper no. 72 in this compilation).

Schueller, Carl F.: Interactions Between the External Flow and Rocket Exhaust Nozzle. Paper no. 59-133, Inst. Aeronautical Sci., Oct. 1979.